(-)-Epicatechin Inhibits Cardiac Fibrosis via SIRT1/AKT/GSK3β Pathway

Yuanyuan Guo
First Affiliated Hospital of Harbin Medical University
Yingchun Luo
First Affiliated Hospital of Harbin Medical University
Zeng Wang
First Affiliated Hospital of Harbin Medical University
zengxiang dong (dongzx1982@163.com)
The First Affiliated Hospital of Harbin Medical University https://orcid.org/0000-0001-5255-3270
Yue Li
First Affiliated Hospital of Harbin Medical University

Research

Keywords: (-)-Epicatechin, cardiac fibrosis, SIRT1, AKT, GSK3β

Posted Date: May 10th, 2021

DOI: https://doi.org/10.21203/rs.3.rs-484230/v1

Abstract

Background: (-)-Epicatechin (EPI) is an important substance involved in protective effects of flavanol-rich foods. Many studies indicate EPI has cardioprotective effect, but the effect of EPI in inhibition of cardiac fibrosis is unclear. Thus, we aimed to evaluate the effect of EPI in preventing cardiac fibrosis and unveil the molecular mechanisms.

Methods: Cardiac fibrosis model was established by transaortic constriction (TAC). The acutely isolated cardiac fibroblasts were induced to myofibroblasts with angiotensin II (AngII).

Results: EPI markedly attenuated TAC-induced cardiac dysfunction and fibrosis in mice. In cultured CFs, EPI blocked AngII-induced myofibroblast transformation and collagen production. Furthermore, EPI conducted anti-fibrotic effects by activating the the SIRT1/AKT/GSK3β pathway.

Conclusions: These findings will supply new agent and mechanism of action for treating cardiac fibrosis in the future.

Introduction

Cardiac fibrosis is the key pathophysiological process in cardiac remodeling and heart failure [1, 2]. Cardiac fibroblasts (CFs) can be transformed into myofibroblasts by pathological stress [3]. There is a potential treatment for inhibiting cardiac fibrosis by suppressing myofibroblasts transformation. (-)-Epicatechin (EPI), extracted from many flavanol-rich substances, including cocoa and green tea, which is known as an important constituent exerted protective effects on cardiovascular system [4-7]. The above of these studies focused especially on role of EPI in cardiac function. The specific action of EPI on cardiac fibrosis remains unclear, and exact mechanism of EPI regulating pathway in cardiac fibroblasts needs to be determined.

SIRT1, a member of the sirtuin family of nicotinamide adenine dinucleotide (NAD+)- dependent histone deacetylases, not only involved in regulating oxidative stress and inflammatory, but also played a protective role in organ fibrosis [8-10]. Previous study found that activation of SIRT1 could prevent cardiac fibrosis [11]. Recently, lots of studies found that EPI could mediate activation of SIRT1 in hepatic and endothelial cell [12, 13]. But whether SIRT1 participating in EPI-inhibited cardiac fibrosis is unclear. Glycogen synthase kinase-3β (GSK-3β), a member of serine/threonine kinase family which regulated various cellular physiology [14]. Meantime, GSK-3β played an important role in cardiac physiology. Moreover, GSK-3β could be phosphorylated by AKT (protein kinase B, a multifunctional protein kinase), which showed cardioprotective effect [14].

Therefore, our aim was to evaluate the protective effect of EPI on cardiac fibrosis and elucidate the exact mechanism. Through established cardiac fibrosis model in vivo and in vitro, we demonstrated an antifibrotic effect of EPI on cardiac fibrosis, and SIRT1/AKT/GSK3β pathway participated in EPI inhibiting cardiac fibrosis.

Methods

Animal model and treatment

Mice were fed though freely available diet for 7 days acclimatization under normal room temperature and humidity conditions. Mice were then randomly separated into sham/control, EPI (1mg/kg/day), transaortic constriction (TAC), and TAC+EPI (1 mg/kg/day) groups. The dose selection of EPI was conformed in accordance with previous study [15]. Tribromoethyl alcohol (20 mg/kg, i.p., MCE, USA) were used to anaesthetize mice. TAC was conducted as previous study [16]. Intragastric administration of EPI was conducted in mice for 28 days. Equal volume of saline was given into control group animals. Animal experiments approved by the Institutional Animal Care and Use Committee of Harbin Medical University and were complied with Guide for the Use and Care of Laboratory Animals published by National Institutes of Health (NIH Publication No. 85-23, revised 1996).

Echocardiographic measurement

Echocardiography of cardiac structure and function was determined as previously reported [17]. Echocardiographic measurement were conducted with ultrasonic echocardiographic instrument (Visualsonic Vevo 1100, Canada). The cardiac parameters of five mice were measured in each group after 28 days of TAC or treatment.

Histological analysis

Histological analysis of mice's hearts were determined with H&E or Masson method. The myocardial sections were observed by microscope (Carl Zeiss Co. Ltd., USA). Collagen deposition was evaluated with collagen volume fraction (CVF). HW/BW index was calculated using mouse heart weight to body weight ratio.

Cell culture

Cardiac fibroblasts (CFs) were acutely isolated from neonatal SD rats (1-3-day-old). CFs were cultured in routinely conditions (37 °C, 5 % CO_2). The cells were divided into different groups and subjected to experimental procedures at 80 % confluence. According to experimental group, CFs were treated with 10 μM AngII or / and 10 μM EPI for 24 h.

Small interference RNA (Si-RNA) transfection

CFs were transfected with SIRT1 Si-RNA or NC Si-RNA (Genechem, Shanghai, China). The SIRT1 and NC Si-RNA sequences: SIRT1, sense 5'-GATCCCA CCCTGTAAAGCTTTCAGAAACTCGAGTTTCTGAAAGCTTTACAGGGTTTTTTGGAT-3' and antisense 5'-AGCTATCCAAAAAACCCTGTAAAGCTTTCAGA AACTCGAGTTTCTGAAAGCTTTACAGGGTGG-3'; and NC, sense 5'-GATCCCT TCTCCGAACGTGTCACGTCTCGAGACGTGACACGTTCGGAGAATTTTTGGA T-3' and antisense 5'-AGCTATCCAAAAA TTCTCCGAACGTGTCACGTCTCG AGACGTGACACGTTCGGAGAAGG-3'.

After CFs had grown to 80% confluence on 60mm dish, transfection was accomplished by using GoldenTran®-DR.

Western blot analysis

Cell protein was extracted from CFs under different given condition for analysis. The blots were probed with primary antibody including α-SMA (Santa Cruz, USA), COLI/COLIII (Santa Cruz, USA), SIRT1 (Abcam, USA), AKT/Phospho-AKT (Santa Cruz, USA), GSK3β/Phospho-GSK3β (Santa Cruz, USA), and GAPDH (Zsgb, China). The blots were probed with secondary antibody (Zsgb, China). The bands were detected by imaging instrument (LI-COR, USA).

Immunofluorescence assay

Briefly, CFs were stained with α-SMA antibody for 12h. Cells were washed with PBS. Then, secondary antibody (Molecular Probes, Invitrogen) was added for 1 h. DAPI was added for 3 min. Immunofluorescence were detected by microscope (Carl Zeiss , USA). The magnification is ×200.

Statistical analysis

Results were shown as the mean ± SEM and analyzed with SPSS 20.0 statistical software. Difference comparisons were determined using one-way ANOVA and considered to be statistically significant when $P < 0.05$.

Results

EPI prevents cardiac fibrosis

To examine whether EPI protects heart against cardiac fibrosis, we firstly established the TAC mouse models. Then intragastric administration of EPI was conducted into mice for 28 days after established TAC models. Echocardiography was used to monitor the cardiac function (Figure 1). LVEF, LVFS, LVIDs, LVIDd, LVPWs, LVPWd, IVSs and IVSd were detected. Compared to control group, TAC decreased LVEF, LVFS and increased LVIDs, LVIDd, which were ameliorated by EPI treatment.

The protective effect of EPI on the TAC-induced alteration of cardiac structure was determined. As shown in Figure 2, the results showed that collagen content was increased in the heart tissues of TAC group, which was significantly reduced by EPI treatment (Figure 2A-C). In addition, administration of EPI substantially reduced HW/BW index in TAC group (Figure 2D).

EPI blocks AngII-induced myofibroblasts transformation

To examine whether EPI protects cardiac fibroblast (CFs) against AngII-induced myofibroblasts transformation, we used primary cultured neonatal rat cardiac fibroblast for vitro models of cardiac fibrosis. Cells were incubated using Ang II or/and EPI for 24 h. As indicated in Figure 3A-B, α-SMA-positive

area was significantly increased in AngII-treated group, and EPI inhibited AngII-induced fibroblast transformation.

To further evaluate protective effect of EPI on cardiac fibrosis, protein of α-SMA and collagenI/III (COLI/III) were detected by western blot (Figure 3C-E). As we expected, Ang II increased the protein expression of α-SMA and COLI/III. EPI efficiently inhibited these changes, suggesting that the myofibroblasts transformation and collagen synthesis induced by AngII could be mitigated by EPI.

EPI activates SIRT1/AKT/GSK3β pathway

To determine the signaling pathway participated in EPI-blocked myofibroblasts transformation, we studied the effect of EPI on the protein expression of SIRT1, AKT, GSK3β, P-AKT and P-GSK3β (Figure 4). As shown in Figure 4A-C, western blot analysis indicated EPI significantly increased the protein expression of SIRT1, P-AKT and P-GSK3β in CFs.

Next, we explored whether SIRT1 participates in EPI-induced activation of AKT/GSK3β. As shown in Figure 4D, EPI increased the protein level of SIRT1. We used Si-RNA approach to knock down SIRT1, which blocked SIRT1 proteins increased by EPI. We tested whether knockdown of SIRT1 could affect activation of AKT/GSK3β induced by EPI. As we expect, knockdown of SIRT1 significantly decreased protein level of P-AKT and P-GSK3β (Figure 4E-F), which illustrated that EPI-induced activation of AKT and GSK3β was mediated by SIRT1. These data suggested that EPI might activate SIRT1/AKT/GSK3β pathway for inhibiting cardiac fibrosis. These observations also found that SIRT1/AKT/GSK3β pathway was not affected by AngII.

SIRT1 participates in EPI-inhibited myofibroblasts transformation

Furthermore, as SIRT1 has been shown to participate in EPI-induced activation of AKT and GSK3β, we tested whether SIRT1 was involved in EPI-inhibited myofibroblasts transformation. We used Si-RNA approach to knock down SIRT1, which removed SIRT1, P-AKT and P-GSK3β proteins increased by EPI, and abolished the protective role of EPI against AngII (Figure 5A-C).

Next, we used Si-RNA approach to knock down SIRT1 in CFs. Then cells were incubated using Ang II or/and EPI for 24 h. As indicated in Figure 6A-B, α-SMA-positive area was significantly decreased in EPI+AngII-treated group, and Si-SIRT1 blocked EPI-inhibited myofibroblasts transformation. These results even further suggested that SIRT1 was essential for EPI-induced activation of AKT and GSK3β, which was also required for EPI-inhibited myofibroblasts transformation.

Discussion

The protective effect and mechanism of EPI on cardiac fibrosis was identified in this study. We found that EPI could alleviate cardiac fibrosis. The anti-fibrosis mechanism of EPI might be conducted via the SIRT1AKT/GSK3β signaling. The previous study found that flavanol-rich foods such as EPI and epigallocatechin-3-gallate (EGCG) had cardioprotective effects [6, 18]. EPI could protect cardiovasculature

through reducing arginase expression and increasing NOS expression [19, 20]. Furthermore, EPI protected myocardial ischemia induced-cardiac injury through activation of PTEN/PI3K/AKT signaling [15]. There were many studies had reported that EGCG cloud ameliorate cardiac hypertrophy and fibrosis [21, 22]. In our study, we found that EPI could improve heart function and reduce cardiac fibrosis in hearts of TAC mice and inhibit AngII-induced α-SMA and COLI/III expression.

SIRT1 could inhibit oxidative stress and inflammatory, and attenuate cardiac fibrosis [11]. In our study, we found EPI up-regulated protein level of SIRT1. Moreover, EPI could also up-regulate protein level of P-AKT and P-GSK3β. Previous studies found that GSK3β mediated in regulation of several signaling proteins [23, 24]. GSK3β also involved in activation of CFs and cardiac remodeling [24]. AKT/GSK3β pathway played a pivotal role in regulating cell proliferation and apoptosis [25]. Furthermore, the activation of SIRT1 and AKT signaling could prevent cardiac fibrosis in post-myocardial infarction [26]. In our study, we observed that knock down SIRT1, which removed SIRT1 proteins, significantly decreased protein level of P-AKT and P-GSK3β, and blocked EPI-inhibited myofibroblasts transformation. These data deeply indicated that SIRT1 involved in EPI-induced activation of AKT/GSK3β, which was also required for EPI-inhibited myofibroblasts transformation. In our study, AngII did not affect SIRT1/AKT/GSK3β pathway. The previous study indicated that AngII could induce myofibroblasts transformation though TGFβ1-SMAD3 pathway [27]. The activation of GSK3β could inhibit the TGFβ1-SMAD3 pathway [28]. So, our results indicate that EPI-induced activation of AKT/GSK3β maybe inhibit the AngII/TGFβ1-SMAD3 pathway for reducing myofibroblasts transformation. The follow-up mechanism needs further study.

Conclusions

In summary, our study indicates that EPI can prevent cardiac fibrosis. SIRT1/AKT/GSK3β pathway mediates EPI-inhibited cardiac fibrosis. These findings will supply new agent and mechanism of action for treating cardiac fibrosis in the future.

Abbreviations

EPI: (-)-Epicatechin; SIRT1: Sirtuin1; AKT: Protein kinase B; GSK3β: Glycogen synthase kinase 3β; CFs: cardiac fibroblasts; TAC: transaortic constriction; AngII: angiotensin II; LVIDs: left ventricular systolic internal diameter; LVIDd: left ventricular diastolic internal diameter; LVPWs: left ventricular posterior wall thickness in systole; LVPWd: left ventricular posterior wall thickness in diastole; LVEF: left ventricular ejection fraction; LVFS: left ventricular fractional shortening; IVSs: interventricular septal thickness at end systole; IVSd: interventricular septal thickness at end diastole; HE: hematoxylin and eosin; HW/BW: heart weight/ body weight ratio.

Declarations

Ethics approval and consent to participate

Not applicable.

Consent for publication

All authors have given their consent for the manuscript to be published.

Availability of data and materials

The datasets used and/or analyzed during the current study are available from the corresponding author on reasonable request.

Declaration of competing interest

The authors declare that there is no conflict of interest.

Funding

The study was funded by the National Natural Science Foundation of China (No. 81870169, 81400250, 81900366), Natural Science Foundation of Heilongjiang Province (H2017040), Postdoctoral Initiation Foundation of Heilongjiang Province (LBH-Q19032).

Author's contributions

Designed and conceived study: ZXD, YL. Performed experiments: YYG, YCL, ZW. Analyzed data: YCL, ZW. Wrote manuscript: YYG, YCL. Overall responsibility: ZXD, YL.

Acknowledgements

Not applicable.

References

1. Braunwald E. Heart failure. JACC Heart Fail 2013; 1: 1-20.
2. Shah AM, Mann DL. In search of new therapeutic targets and strategies for heart failure: recent advances in basic science. Lancet 2011; 378: 704-712.
3. Travers JG, Kamal FA, Robbins J, Yutzey KE, Blaxall BC. Cardiac Fibrosis: The Fibroblast Awakens. Circ Res 2016; 118: 1021-1040.
4. Quine SD, Raghu PS. Effects of (-)-epicatechin, a flavonoid on lipid peroxidation and antioxidants in streptozotocin-induced diabetic liver, kidney and heart. Pharmacol Rep 2005; 57: 610-615.
5. Yamazaki KG, Romero-Perez D, Barraza-Hidalgo M, Cruz M, Rivas M, Cortez-Gomez B, Ceballos G, Villarreal F. Short- and long-term effects of (-)-epicatechin on myocardial ischemia-reperfusion injury. Am J Physiol Heart Circ Physiol 2008; 295: H761-767.

6. Yamazaki KG, Taub PR, Barraza-Hidalgo M, Rivas MM, Zambon AC, Ceballos G , Villarreal FJ. Effects of (-)-epicatechin on myocardial infarct size and left ventricular remodeling after permanent coronary occlusion. J Am Coll Cardiol 2010; 55: 2869-2876.
7. Taub PR, Ramirez-Sanchez I, Ciaraldi TP, Perkins G, Murphy AN, Naviaux R, Hogan M, Maisel AS, Henry RR, Ceballos G, Villarreal F. Alterations in skeletal muscle indicators of mitochondrial structure and biogenesis in patients with type 2 diabetes and heart failure: effects of epicatechin rich cocoa. Clin Transl Sci 2012; 5: 43-47.
8. Shaikh SB, Prabhu A, Bhandary YP. Targeting anti-aging protein sirtuin (Sirt) in the diagnosis of idiopathic pulmonary fibrosis. J Cell Biochem 2019; 120: 6878-6885.
9. Haigis MC, Sinclair DA. Mammalian sirtuins: biological insights and disease relevance. Annu Rev Pathol 2010; 5: 253-295.
10. Zeng Z, Cheng S, Chen H, Li Q, Hu Y, Wang Q, Zhu X, Wang J. Activation and overexpression of Sirt1 attenuates lung fibrosis via P300. Biochem Biophys Res Commun 2017; 486: 1021-1026.
11. Liu ZH, Zhang Y, Wang X, Fan XF, Zhang Y, Li X, Gong YS, Han LP. SIRT1 activation attenuates cardiac fibrosis by endothelial-to-mesenchymal transition. Biomed Pharmacother 2019; 118: 109227. doi: 10.1016/j.biopha.2019.109227.
12. Cheng H, Xu N, Zhao W, Su J, Liang M, Xie Z, Wu X, Li Q. (−)-Epicatechin regulates blood lipids and attenuates hepatic steatosis in rats fed high-fat diet. Mol Nutr Food Res 2017; 61(11). doi: 10.1002/mnfr.201700303.
13. Ramirez-Sanchez I , Mansour C , Navarrete-Yañez V , Ayala-Hernandez M , Guevara G , Castillo C , Loredo M , Bustamante M , Ceballos G, Villarreal FJ .(−)-Epicatechin induced reversal of endothelial cell aging and improved vascular function: underlying mechanisms. Food Funct 2018; 9: 4802-4813.
14. Sharma AK, Bhatia S, Al-Harrasi A, Nandave M, Hagar H. Crosstalk between GSK-3β-actuated molecular cascades and myocardial physiology. Heart Fail Rev 2020. doi: 10.1007/s10741-020-09961-9.
15. Li JW, Wang XY, Zhang X, Gao L, Wang LF, Yin XH. (-)-Epicatechin protects against myocardial ischemia-induced cardiac injury via activation of the PTEN/PI3K/AKT pathway. Mol Med Rep 2018; 17: 8300-8308.
16. Qin W, Du N, Zhang L, Wu X, Hu Y, Li X, Shen N, Li Y, Yang B, Xu C, Fang Z, Lu Y, Zhang Y, Du Z. Genistein alleviates pressure overload-induced cardiac dysfunction and interstitial fibrosis in mice. Br J Pharmacol 2015; 172: 5559-5572.
17. Luo T, Chen B, Wang X. 4-PBA prevents pressure overload-induced myocardial hypertrophy and interstitial fibrosis by attenuating endoplasmic reticulum stress. Chem Biol Interact 2015; 242: 99-106. .
18. Wu Y, Xia ZY, Zhao B, Leng Y, Dou J, Meng QT, Lei SQ, Chen ZZ, Zhu J. (-)-Epigallocatechin-3-gallate attenuates myocardial injury induced by ischemia/reperfusion in diabetic rats and in H9c2 cells under hyperglycemic conditions. Int J Mol Med 2017; 40: 389-399.

19. MacRae K, Connolly K, Vella R, Fenning A. Epicatechin's cardiovascular protective effects are mediated via opioid receptors and nitric oxide. Eur J Nutr 2019; 58: 515-527.
20. Ortiz-Vilchis P, Ortiz-Flores M, Pacheco M, Ramirez-Sanchez I, Moreno-Ulloa A, Vega L, Ortiz A, Villarreal F, Rubio-Gayosso I, Najera N, Meaney E, Ceballos G. The cardioprotective effects of (-)-Epicatechin are mediated through arginase activity inhibition in a murine model of ischemia/reperfusion. Eur J Pharmacol 2018; 818: 335-342.
21. Muhammed I, Sankar S, Govindaraj S. Ameliorative Effect of Epigallocatechin Gallate on Cardiac Hypertrophy and Fibrosis in Aged Rats. J Cardiovasc Pharmacol 2018; 71: 65-75.
22. Cai Y, Yu SS, Chen TT, Gao S, Geng B, Yu Y, Ye JT, Liu PQ. EGCG inhibits CTGF expression via blocking NF-KB activation in cardiac fibroblast. Phytomedicine 2013; 20: 106-113.
23. MacAulay K , Woodgett JR. Targeting glycogen synthase kinase-3 (GSK-3) in the treatment of type 2 diabetes. Expert Opin Ther Targets 2008; 12: 1265-1274.
24. Liu X, Liu C, Li J, Zhang X, Song F, Xu J. Urocortin attenuates myocardial fibrosis in diabetic rats via the Akt/GSK-3β signaling pathway. Endocr Res 2016; 41: 48-57
25. .Dai J, Qian C, Su M, Chen M, Chen J. Gastrokine-2 suppresses epithelial mesenchymal transition through PI3K/AKT/GSK3β signaling in gastric cancer. Tumour Biol 2016; 37: 12403-12410.
26. Jia D, Hou L, Lv Y, Xi L, Tian Z. Postinfarction exercise training alleviates cardiac dysfunction and adverse remodeling via mitochondrial biogenesis and SIRT1/PGC-1α/PI3K/Akt signaling. J Cell Physiol 2019; 234: 23705-23718.
27. Zhou HT, Yu XF, Zhou GM. Diosgenin inhibits angiotensin II-induced extracellular matrix remodeling in cardiac fibroblasts through regulating the TGF-β1/Smad3 signaling pathway. Mol Med Rep 2017; 15: 2823-2828.
28. Lal H, Ahmad F, Zhou J, Yu JE, Vagnozzi RJ, Guo Y, Yu D, Tsai EJ, Woodgett J, Gao E, Force T. Cardiac fibroblast glycogen synthase kinase-3β regulates ventricular remodeling and dysfunction in ischemic heart. Circulation 2014; 130: 419-430.

Figures

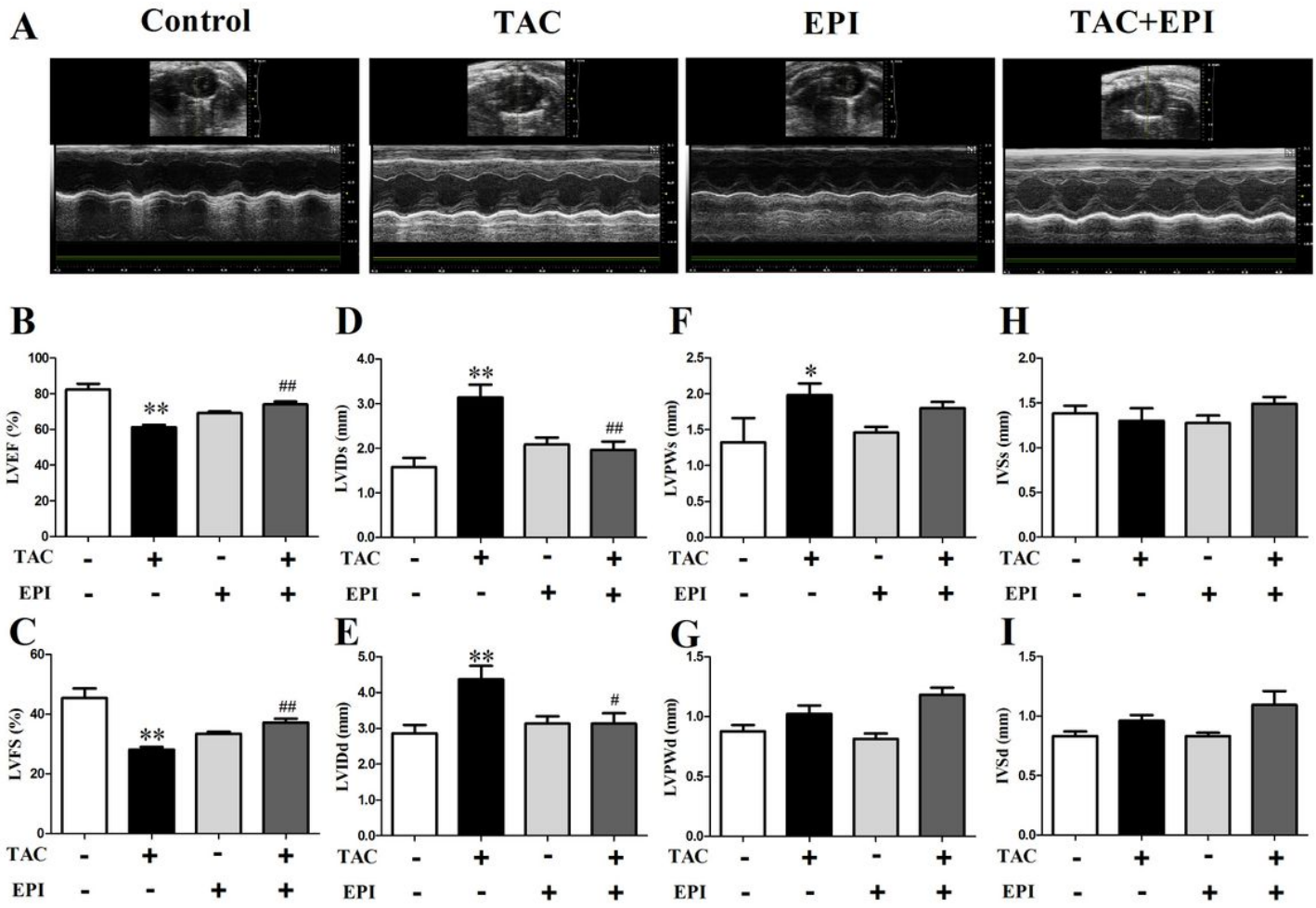

Figure 1

The effect of EPI on cardiac function in mice. (A) Representative cardiac echocardiography of the indicated groups. (B)-(I) LVEF: left ventricular ejection fraction, LVFS: left ventricular fractional shortening, LVIDs: left ventricular systolic internal diameter, LVIDd: left ventricular diastolic internal diameter, LVPWs: Left ventricular posterior wall thickness in systole, LVPWd: left ventricular posterior wall thickness in diastole, IVSs: interventricular septal thickness at end systole, IVSd: interventricular septal thickness at end diastole. Data are shown as mean ± SEM (n=5). *P<0.05, **P<0.01 compared with control group; # P<0.05, ## P<0.01 compared with TAC group.

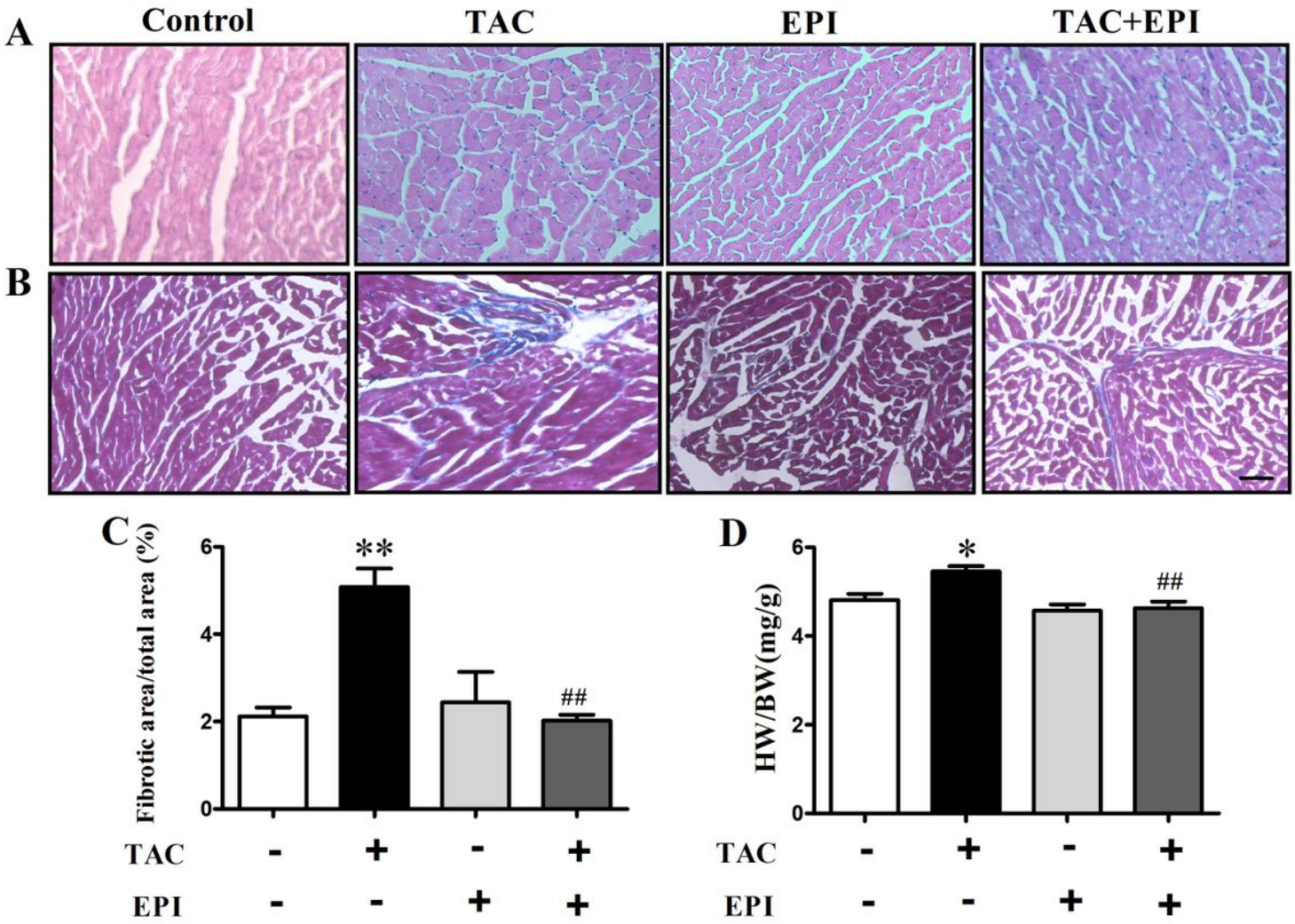

Figure 2

The effect of EPI on myocardial structure in mice. Representative graph of H&E (A) and Masson (B). The magnification is ×200, scale bar = 20 μm. Statistical analysis of collagen deposition (C) and HW/BW index (D). Data are shown as mean ± SEM (n=5). **P<0.01 compared with control group; ## P<0.01 compared with TAC group.

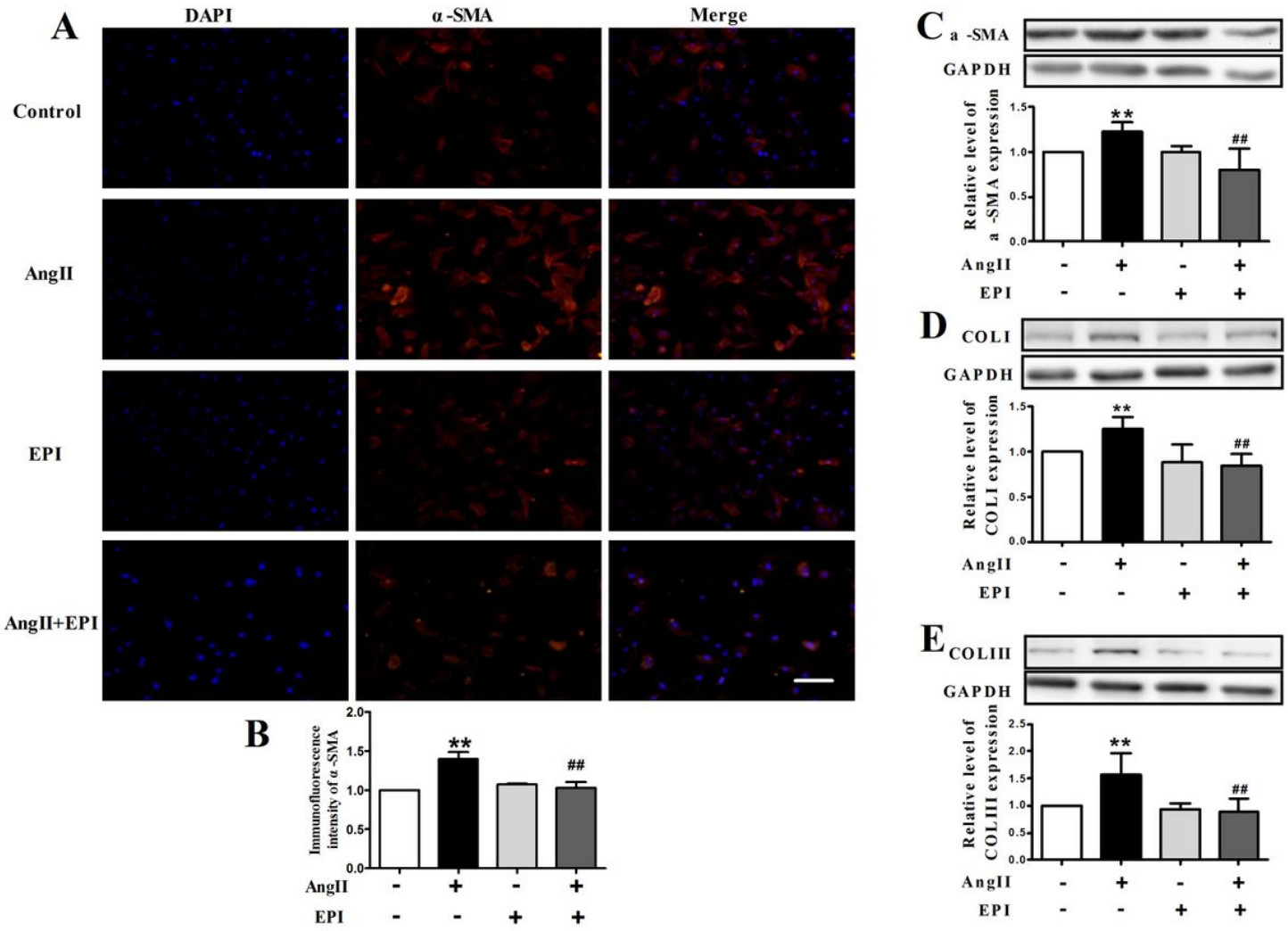

Figure 3

EPI blocks AngII-induced myofibroblast transformation. (A) CFs stained with α-SMA (red) and DAPI (blue) antibody in each group. (B) Statistical analysis of α-SMA. The magnification is ×200, scale bar = 20 μm. (C-E) Western blot bands and statistical analysis of α-SMA, COLI and COLIII after incubation with EPI or/and AngII in CFs. Data are shown as mean ± SEM (n=6). **P<0.01 compared with control group; ## P<0.01 compared with AngII group.

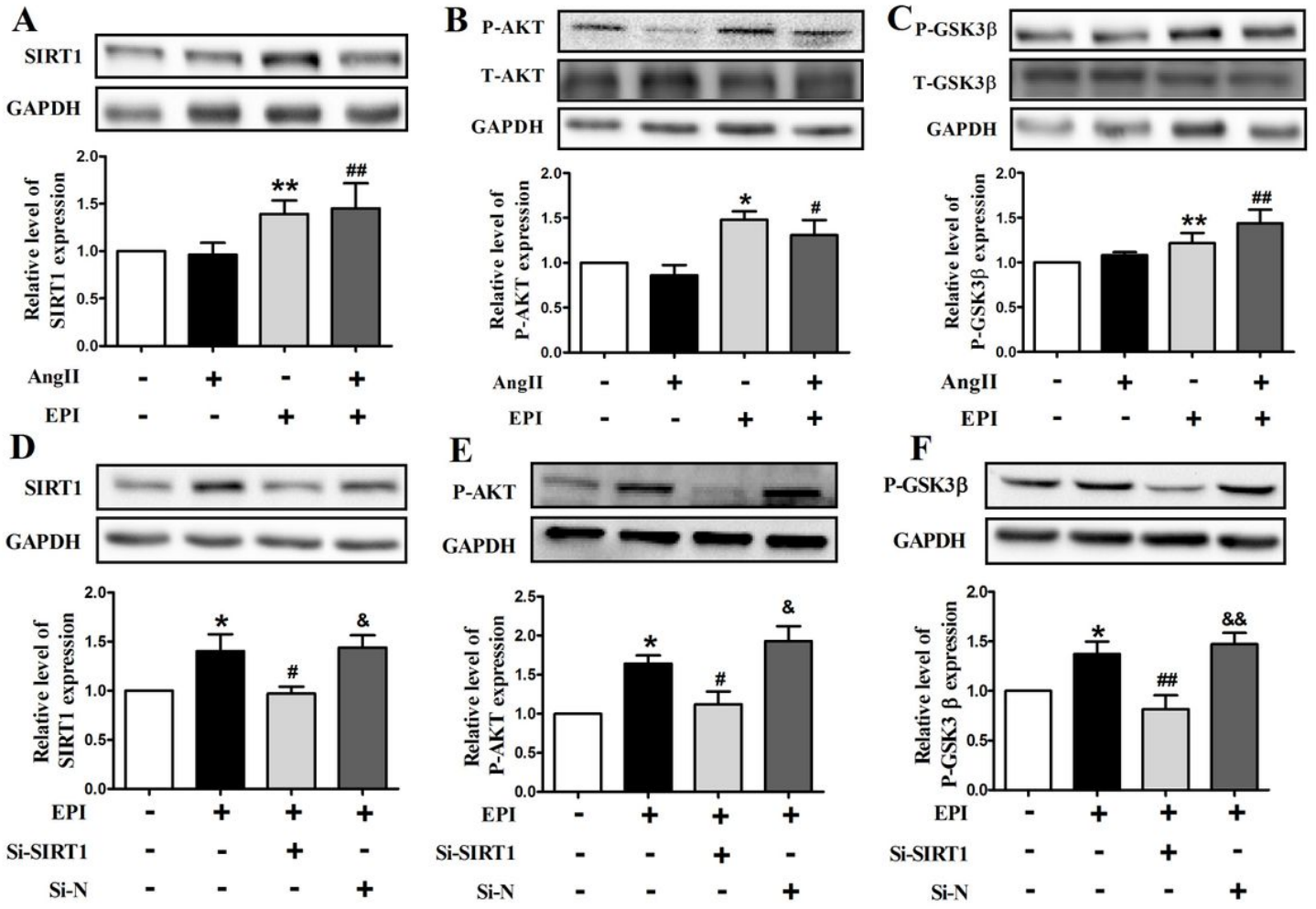

Figure 4

The effect of EPI on protein levels of SIRT1/AKT/GSK3β. (A-C) Representative western blot bands and statistics of SIRT1, AKT/P-AKT and GSK3β/P-GSK3β after incubation with EPI or /and AngII in CFs. (D-F) Representative western blot bands and statistics of SIRT1, P-AKT and P-GSK3β after incubation with EPI or /and Si-SIRT1 in CFs. Data are shown as mean ± SEM (n=6). *P<0.05, **P<0.01 compared with control group; #P<0.05, ##P<0.01 compared with AngII or EPI group. & P<0.05, && P<0.01 compared with EPI + Si-SIRT1 group.

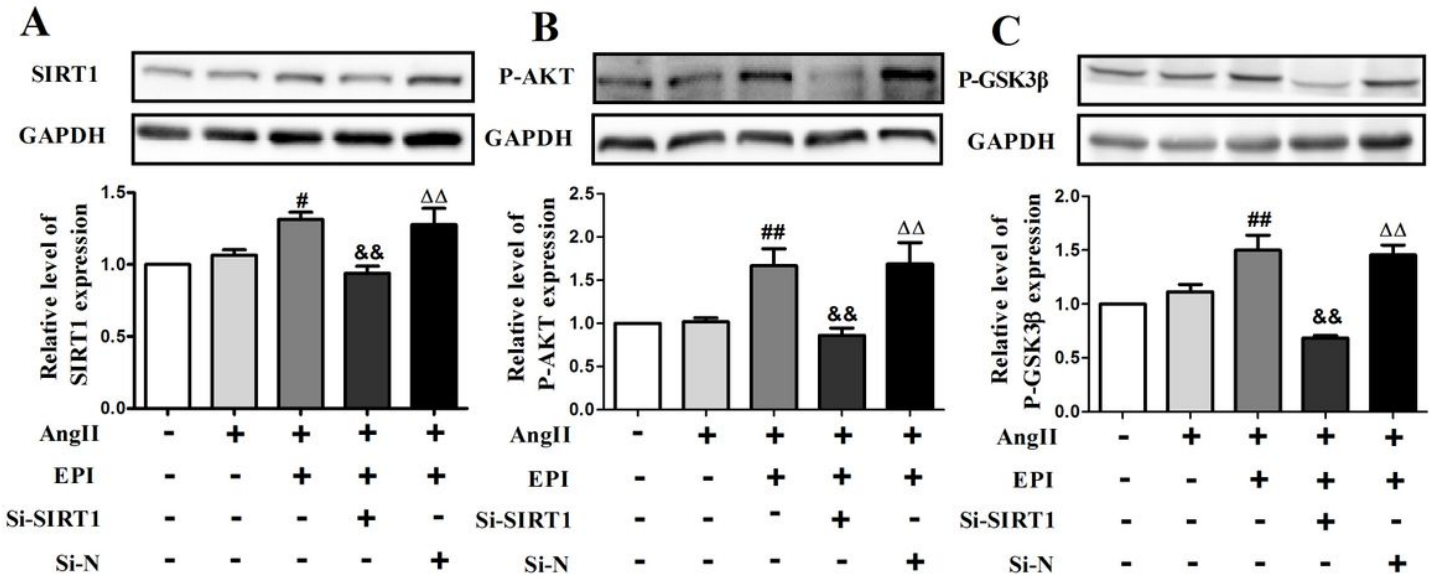

Figure 5

The effect of SIRT1 on EPI-induced protein levels of P-AKT and P-GSK3β. (A) Representative western blot bands and statistics of SIRT1, P-AKT and P-GSK3β after incubation with AngII, EPI, Si-SIRT1 and Si-N in CFs. Data are shown as mean ± SEM (n=6). # P<0.05, ## P<0.01 compared with AngII group; && P<0.01 compared with AngII + EPIgroup. △△P<0.01 compared with AngII + EPI + Si-SIRT1 group.

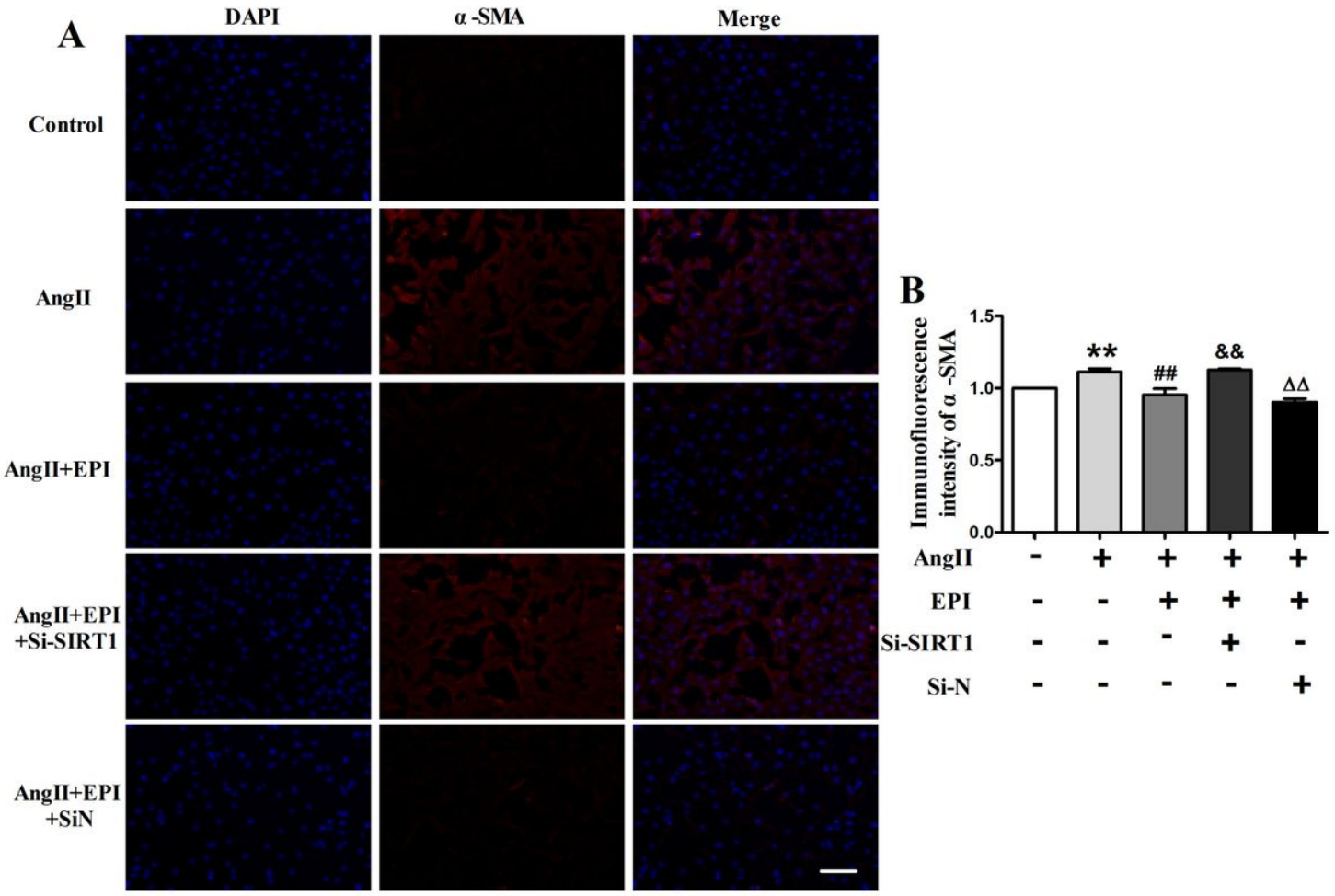

Figure 6

The effect of SIRT1 on myofibroblast transformation. (A) CFs stained with α-SMA (red) and DAPI (blue) antibody in each group. (B) Statistical analysis of α-SMA. The magnification is ×200, scale bar = 20 μm. Data are shown as mean ± SEM (n=6). **P<0.01 compared with control group; ##P<0.01 compared with AngII group; &&P<0.01 compared with AngII + EPI group; △△P<0.01 compared with AngII + EPI + Si-SIRT1 group.